applied mechanics

MDPI

Article

An Investigation of the Effects and Consequences of Combining Expanding Dual Pin with Radial Spherical Plain Bearings

Øyvind Karlsen [1,2,*], Hirpa G. Lemu [1,*] and Imad Berkani [2]

[1] Faculty of Science and Technology, University of Stavanger, 4021 Stavanger, Norway
[2] Bondura Technology AS, 4340 Bryne, Norway; imad@bondura.no
* Correspondence: oyvind.karlsen@uis.no or oyvind@bondura.no (Ø.K.); hirpa.g.lemu@uis.no (H.G.L.)

Abstract: An expanding pin locks the pin assembly to its supports and bearings and prevents any relative movements between the surfaces in contact. In this study, the diameter changes of the bearing inner ring as a function of the expanding pin's tightening torque were studied. In addition, the required rotational moment of a set of complete bearings locked to an expanding pin solution was studied by exposing the assembly to a combination of an increasing radially outwards directed load from the bolt torquing and a radially external inwards directed load from a hydraulic jack. The bearings were of type Radial Spherical Plain Bearings (RSPBs), GE 80 ES, steel/steel, and loaded externally up to their maximum dynamic limit of 400 kN. The results indicate a major reduction in the required rotation moment of the bearing when the bearing inner ring is expanded by use of an expanding pin. The reduction of rotation moment indicates reduced contact pressure and friction force between the two bearing rings, which ultimately can have a reduced effect on ring surface wear and a positive effect on the bearing operational lifetime.

Keywords: expanding pin; dual pin; radial load; bearing capacity; spherical bearing; bearing wear; bearing lifetime

Citation: Karlsen, Ø.; Lemu, H.G.; Berkani, I. An Investigation of the Effects and Consequences of Combining Expanding Dual Pin with Radial Spherical Plain Bearings. *Appl. Mech.* **2022**, *3*, 573–589. https://doi.org/10.3390/applmech3020034

Received: 28 March 2022
Accepted: 6 May 2022
Published: 10 May 2022

1. Introduction

A moveable joint will often contain minimum two counterparts that turn relative to each other, ideally around a center line in common. The joint can have a female part, a fork, and a male part, together with typically a bearing. Moveable joints are in use in uncountable numbers of different applications, in most industries globally and many different machines and mechanical equipment [1]. In addition, bearings are used in static joints in civil engineering and constructions. By applying a moveable joint, it is possible to transfer heavy loads of any equipment from one position to another or turn rotational movements into axial directional movements [2]. The moveable joints in general can be found in many well-known and familiar tools and furniture, like scissors, garden shears, and rotating chairs, as well as in more industrialized tools, equipment, and machines. Efficient, safe, and well-working moveable joints are indispensable in most industrial equipment and machines such as offshore and onshore cranes, drilling and pipe handling equipment, excavators, dumper trucks and other vehicles for earth moving, windmill systems, flood control gate ports, and even launch platforms for spaceships and rockets. [3]. In addition to the two counterparts that turn relative to each other [4], a third component is required to make a joint moveable, which could be a pin connection with female and male parts as shown in Figure 1a,b. The pin in a moveable joint can be of many different designs, with different advantages or disadvantages. In general, it is an advantage to have as tight tolerance as possible between the pin and the female part (supports), and against the male part during operation of the machine, to avoid any unwanted movements of a cylindrical pin (Figure 1c), which can result in mechanical wear and increased play. At the same time, it is an advantage to have wider tolerances [5] during installation and retrieval

of the pin, to avoid the pin getting stuck in the supports. The different pin designs value differently the tightness of the tolerance, either very tight to increase the quality of the joint during operation, or less tight to ease installation and retrieval of pins. It is common to lubricate the pin and the bore inner surface to reduce friction between surfaces in contact for installation and retrieval purposes [5] and to protect against oxidation, but it is not always required. Such lubrication is typically made of petroleum hydrocarbon distillate with additives to get the specific and required properties.

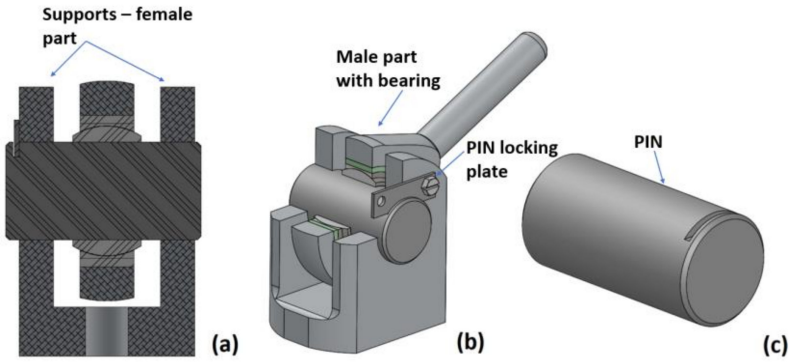

Figure 1. Pin joint illustrated as: (**a**) cross-sectional view, (**b**) isometric view, and (**c**) a cylindrical pin.

The aim of the study reported in this paper is to investigate the effects and consequences of locking an expanding bondura® Dual Pin (Bondura Technology AS, Bryne, Norway) to the inner ring of a Radial Spherical Plain Bearing (RSPB) and compare that with the use of a standard cylindrical pin, for both dry and lubricated contact surfaces. As part of the experimental work, the bearing inner ring is separated from the outer ring and loaded separately with a pressure load acting radially outwards, and its deformations are measured by a Coordinate-Measuring Machine (CMM) to find the relationship between the radial load and the corresponding ring deformation. In addition, the complete bearing with lubricated internal surfaces was installed on a Dual pin and then loaded stepwise with combinations of radial outward force from the expanding sleeve and external inwards radial load representing operational loads. The assembly was then forced to turn, and the required static moment at the exact moment of turning was observed.

2. Literature Review

Traditionally, mechanical joints for load transfer are designed with interference fitting such as shrink fitting and press fitting or using standard cylindrical pins, while expanding pin solutions are more innovative solutions with wide installation tolerances.

Shrink fitting [6] is a method to shrink a slightly oversized pin, by cooling it down with frozen nitrogen, and introduce it into the joint and let it expand back to its normal temperature, at which the interference fit is produced with the contacting support bore surfaces. This solution has a wider installation tolerance and zero operational tolerance between the surfaces in contact. Shrink fitting as a method for joining two mechanical parts has been investigated over many years, e.g., McMillan et al. [7] studied the slip between a hub and a shaft in a shrink-fit assembly subjected to axial load, and Mouaa et al. [8] reported an analytical methodology to analyze the elastic-plastic stresses in a shrink fit with a solid shaft.

Press fitting is another method of interference fitting where a slightly oversized pin is assembled into the female part by applying an axial external load. In this method, the pin is forced into correct position in the joint, reaching the interference fit with the contacting surfaces. This solution has negative/zero installation tolerance and zero operational tolerance, and the performance of this method has been studied both numerically, analytically, and experimentally over the years [9,10].

The most common solution is using *a standard cylindrical pin* joint, where a massive cylindrical dowel pin with a wide enough installation tolerance is used to install the pin without interference. This solution has a wider installation tolerance, which also is the operational tolerance and is often provided with a locking plate installed to prevent the pin from falling out over time.

The expanding pin solution [11,12] is less known but combines the wide installation tolerance from the standard pin solution, and often even wider, with the zero operational tolerance from the shrink fit and press fit solutions. There is a variety of different expanding pin solutions depending on the issues to be addressed, where most of them can expand to zero operational tolerance against the supports. The dual pin solution [11], however, expands in addition against the bearing, to a zero operational tolerance. The operational and damage mechanisms and the advantages of this solution are not sufficiently addressed in the literature. In the recent works of the authors, however, some research results have been reported. For instance, the expanding pin solution, as a part of a mechanical joint, has been compared to other known joint models and modelling techniques, by Karlsen and Lemu [13,14], with focus on the damage mechanisms that can occur in various connections of mechanical systems, typically such as fretting wear, fretting corrosion, and fretting fatigue. In addition, Akhtar et al. [15] reported a study on the capacities of a pin with the combination of radially expanding and axially pre-load capabilities, typically for huge flange systems. Berkani et al. [16] performed an experimental and numerical study of expanding pins with the aim of knowing more about the relation between the tightening torque and stresses generated at the contact surfaces, in addition to the effects of variations in temperature over time.

Öztürk et al. [17] performed an experimental test to determine the coefficient of static friction (COFs) for RSPBs, for polyoxymethylene (POM)/steel contact surfaces. The bearing was exposed to increasing external radial inwards directed load, and the bearing inner ring was turned relative to the outer ring and the COFs values calculated. They concluded that whereas the static friction force increased with increasing normal force, the coefficient of static friction decreased until it stabilized. Zhao et al. [18] investigated failure behaviors of RSPB joints for use in civil engineering applications, and the main findings were brittle fracture of the inner ring and brittle crack of the outer ring under uniaxial radial load, when the pin shaft bent due to overload. Under such loading conditions, the inner ring would have pressure from the outer ring at a limited width around its center line, due to difference in outer ring inner diameter and inner ring outer diameter, but reduced or missing support from the pin shaft around the same center line, due to the bending of the pin. This will result in bending of the inner ring and additional stresses and finally brittle fracture of the edges. Sun et al. [19] studied the use of RSPBs in joints in a space truss structure, subjected to tension and compression, to verify the bearing's mechanical properties and reliability. Fang et al. [20] developed a theoretical solution and a numerical model for conformal contact pressure and free-edge effects in spherical plain bearings, which varies with the bearing clearance and external load.

In the global market, only a few companies produce expanding pin solutions, and to the authors' knowledge, only one company produces the double sets of expanding sleeves, called Dual pins, for locking a second set of expanding sleeves to the bearing. The stakeholders' opinions, experiences, and the use of expanding pins on the global arena have been investigated by Karlsen and Lemu [21,22].

2.1. Expanding Pins

A typical expanding pin assembly, illustrated in Figure 2, has (1) a load bearing pin with conically machined tapered ends, (2) conically machined end-sleeves to fit the tapered pin ends, and (3) end plates and tightening screws or nuts. In addition, the assembly can have lubrication channels, if required. When torquing the screws or nuts, the end-sleeve climbs on the tapered pin end and expands until reaching a zero tolerance between the sleeve and the support bore and produces then a wedge force. The contact pressure between

the support bore and the sleeve, and between the sleeve and the pin, prevents the pin assembly from rotating or displace axially and thereby prevents any unwanted surface wear, ovality issues, etc. The Dual expanding pin can produce a similar wedge lock against the bearing inner ring by a second inner set of expanding sleeves.

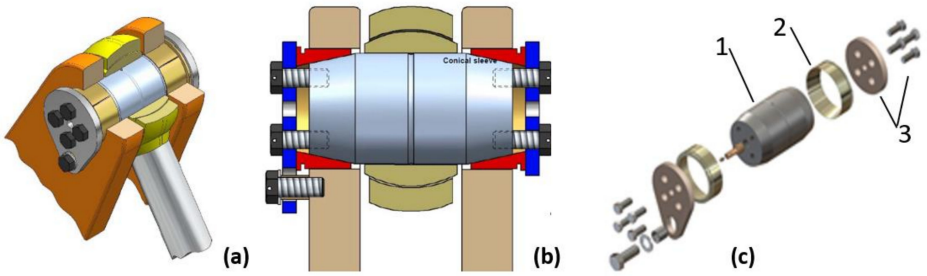

Figure 2. Expanding pin with single set of sleeves: (**a**) pin in joint, (**b**) cross-section view, and (**c**) exploded view.

2.2. Dual Expanding Pins

The Dual expanding pin solutions, illustrated in Figure 3, are applied in various types of industrial cranes offshore or onshore, ports, drilling and pipe handling equipment, rotating sheaves, amusement equipment, A-frames (Figure 3a), hatches on ships, flood dike gates, etc., and the pins often interact with bearings [11]. In such applications, the bearings can typically be of spherical plain or rolling type of bearings, with the latter divided into ball bearings and roller bearings. The inner sleeve expands towards the inner ring of the bearing but creates normally less contact pressure compared to what the outer sleeve does against the support bore. The contact pressure between the bearing and the expanding sleeve is enough to prevent the bearing inner ring from rotating but not high enough to disturb the bearing's function by expanding the inner ring and eliminate the bearing's radial inner production tolerance. Figure 3b illustrates a dual pin assembly, and Figure 3c illustrates a dual pin where one half is shown with an exploded view.

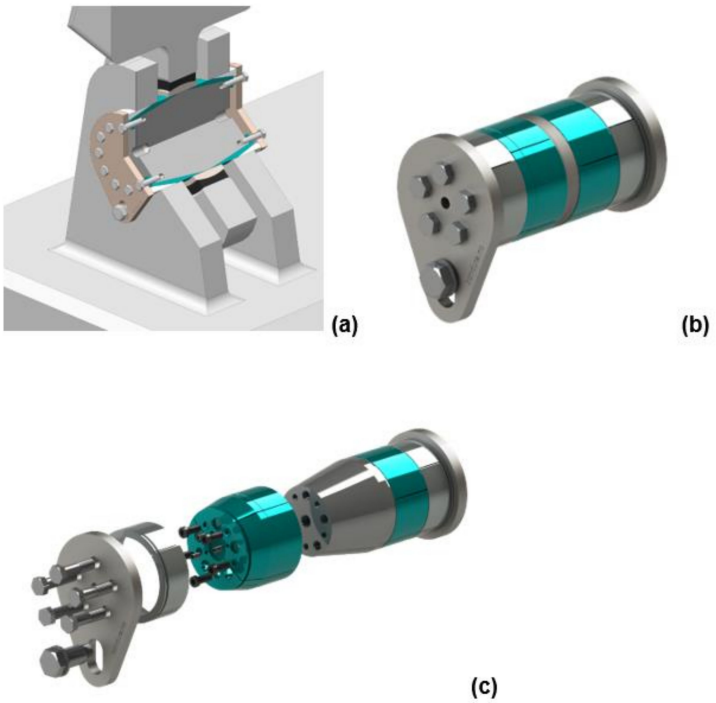

Figure 3. Dual expanding pin with two set of sleeves: (**a**) pin in joint, (**b**) pin assembly and (**c**) exploded view.

3. Materials and Methods

To investigate the performance of the expanding pin solution, both experimental and analytical studies were conducted. The experiments were performed partly at University of Stavanger's (UiS) premises and partly at an external location.

3.1. Experimental Setup

The following two main experimental tests were conducted:

(1) Test 1: tests of bearing inner rings installed on a dual expanding pin;
(2) Test 2: tests of complete bearing assemblies installed on a dual expanding pin.

These tests are detailed in Table 1. Figures 4 and 5 show the test setups for the tests with the Dual Expanding Pin System for Test 1 and Test 2, respectively. For the experimental tests, the bearing inner rings were exposed to outwards radial expansion from an expanding pin solution, and the change of shape was measured by CMM (Zeiss, S/N 532083, Oberkochen, Germany) equipment to find the relation between the bolt tightening torque and the inner ring deformation, specifically the radial deformation.

Table 1. Test setup—pin (Ø80 mm) and bearing combinations.

Bearing Type	Test No.	Number of Rings/Bearings
GE 80 ES (inner ring)	Test 1(a) Test 1(b)	2/2 1/2
GE 80 ES (complete)	Test 2(a) Test 2(b)	0/4 0/3

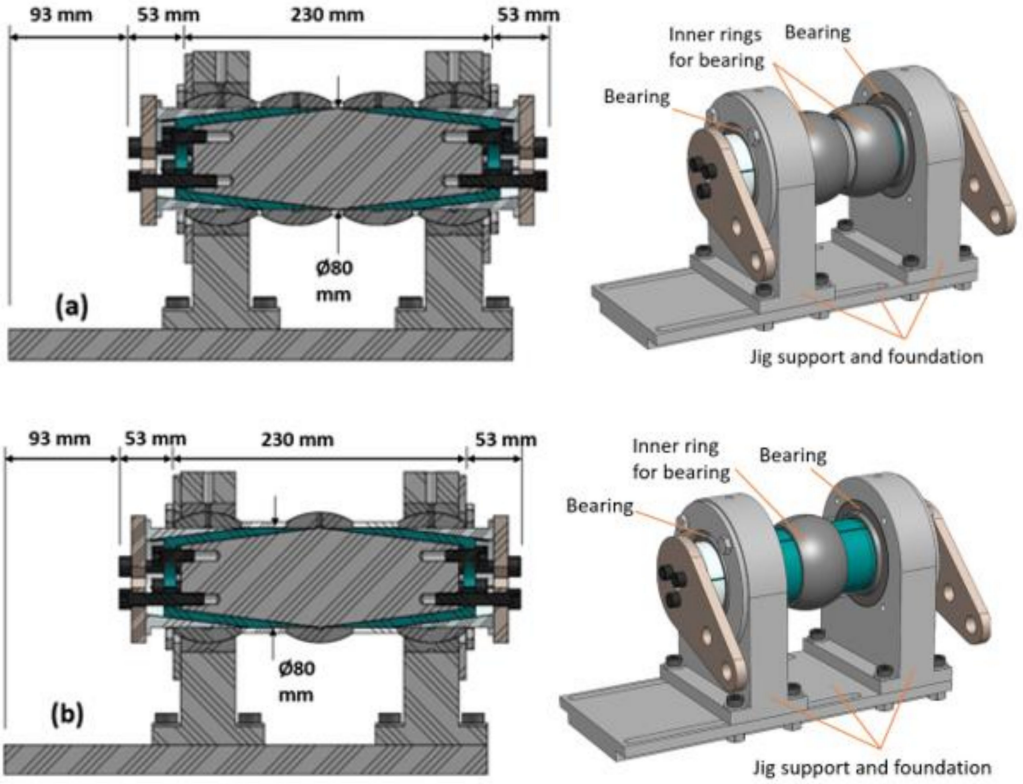

Figure 4. Test setup for Test 1: (**a**) Test 1a—cross sectional view (left) and isometric view with part names (right); (**b**) Test 1b—cross sectional view (left) and isometric view with part names (right).

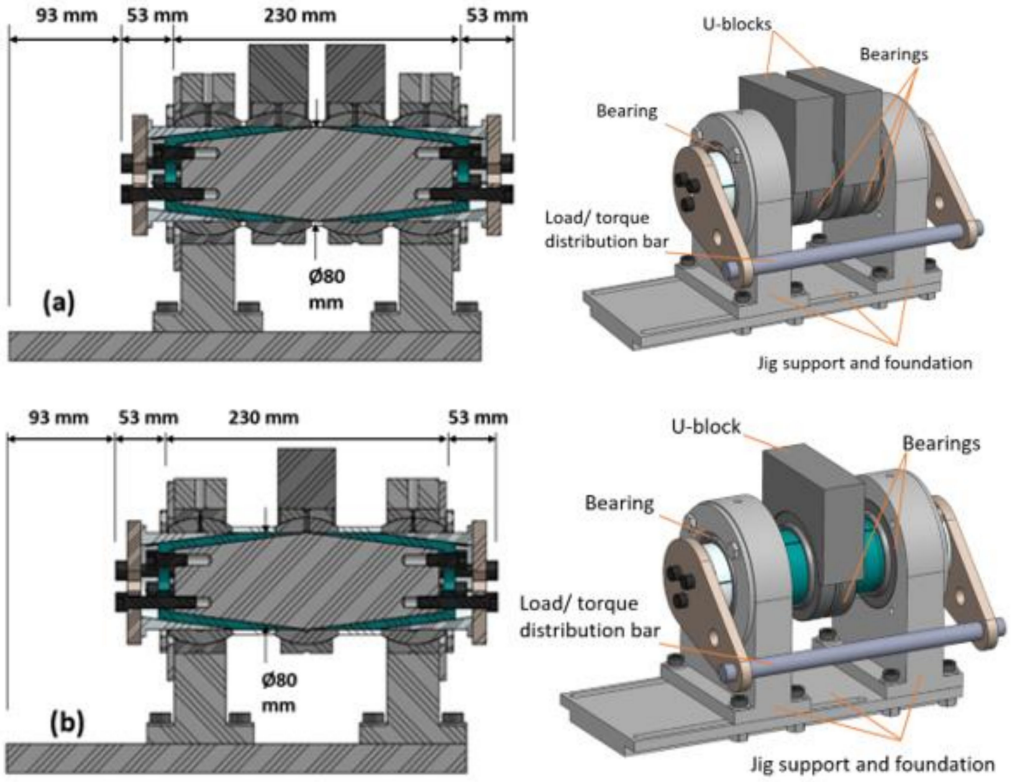

Figure 5. Test setup for Test 2: (**a**) Test 2a—cross sectional view (left) and view with isometric part names (right); (**b**) Test 2b—cross sectional view (left) and isometric view with part names (right).

The three tested inner rings were taken from the bearing SKF GE 80 ES (SKF AS, Oslo, Norway) [23] RSPBs with steel/steel surfaces and metric sizes. The complete bearing set was installed on an expanding pin solution in a test jig and loaded both radially outwards from the expanding pin, in combination with an external load from a 100 tons hydraulic load cylinder (Enerpac, S/N CLP1002E102, Ede, The Netherlands; Urdal Services AS, 4823 Nedenes, Norway). The fabric new bearing internal diameter clearance between the two rings is the range of 72–142 µm, measured perpendicular to the actual pin center axis. The required rotational moment was measured by hydraulically pushing the crossbar (Figure 5) with a 10 tons jack with a force traducer (HBM, S/N 3126849, Darmstadt, Germany) to measure the required load and investigate the effects of the two load combinations on the rotation of the bearings.

The tested GE ES bearings are made of high carbon bearing steel, typically EN 100Cr6/ISO 683-17 [24], through hardened (martensitic) to hardness 57 $\pm$ 2 (HRC), yield limit $R_{p0.2}$ of 2000 MPa, and phosphate treated surface, with Elasticity modulus of 210 GPa and Poisson's ratio of 0.3. The load bearing part of the expanding pin is made of 34CrNiMo6 + QT steel, with yield limit $R_{p0.2}$ of 1003 MPa, and ultimate R_m of 1096 MPa. The expanding inner and outer sleeves are made of 34CrNiMo6 + QT and S355J2 steel, respectively, and the latter sleeve is surface treated with yellow sink plating. The bearings are always internally lubricated to reduce contact friction and to avoid surface damages at the contacting surfaces.

By loading all 4 identical bearings in Test 2a under the same conditions and loads, the total required rotational moment for the assembly will be divided equally between the four bearings. When loading the single bearing in Test 2b, the required rotational moment generated by the two bearings in the supports are known from Test 2a, and the required rotational moment generated by the single bearing is easily calculated.

3.1.1. Bearing Inner Rings Loaded by the Expanding Dual Pin (Tests 1a and 1b)

The Tests 1a and 1b are performed on the inner rings only by introducing a radial outwards force from the expanding dual pin into the inner surface of each ring. The outward directed force is produced by torquing the tightening screws and subsequently pushing the sleeves to move axially and radially until producing a wedge force between the pin and the ring, as indicated in Figure 4. An increment of the screw torque results in an increment in the contact pressure between the sleeve and the inner ring, and the resulting ring dimension changes are measured using the CMM, which is a device that measures the 3D geometry of physical objects by sensing discrete points on the surface of the object with a probe. Various types of probes are used in different CMMs, including mechanical, optical, laser, and white light. The torque on the tightening screws is increased stepwise from zero to a maximum of 70 Nm. For each tightening step, the CMMs measure the ring surface at several points, at four defined cross-section locations, a, b, c and d, at locations −25, −5, +5, and +25 mm respectively, with the zero location at the bearing ring mid-point. For the Test 1a, two inner rings are supported onto one expanding pin sleeve each, giving a full contact surface, except from the lubrication channel with a width of 7.7 mm, towards the rings, as shown in Figure 6a. For the Test 1b, one inner ring is supported onto two separate expanding pin sleeves, giving partly contact surface at the mid-section, against the ring, as indicated in Figure 6b. In the latter test, the ring is not supported at its center part for a width of 12.1 mm, included the lubrication channel, due to distance between the two sleeve ends.

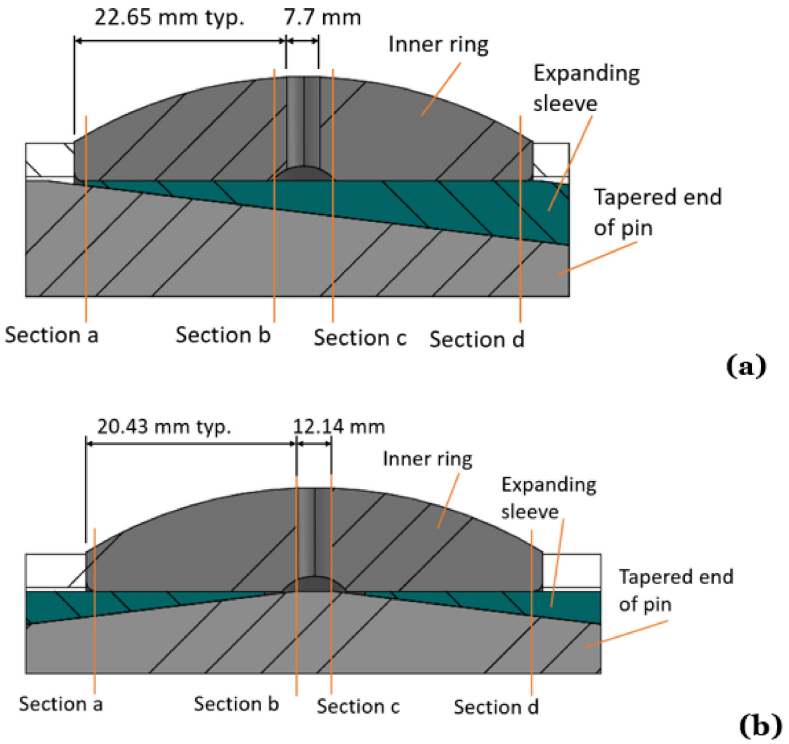

Figure 6. Ring, sleeve, and pin contact area: (**a**) full contact on single sleeve and (**b**) reduced contact at center on double sleeve.

These tests reveal how the inner ring of a complete bearing reacts and deforms when loaded by an expanding pin system, as in Test 2. Tests 1a and 1b are performed both with dry and lubricated (Molykote® P-74, Lindberg & Lund AS, Vestby, Norway) contact surfaces to investigate any effect on the expansion level of the rings, while the bearings in Tests 2a and 2b are performed with lubrication internally (of type SKF LGHB 2), with dry and clean expanding sleeves.

Tests 1a and 1b: The inner rings are separated from the outer rings and exposed directly to outwards radial expansion of the dual pin. One inner ring on one sleeve (Test 1a) and one inner ring on two sleeves (Test 1b). The inner ring deformations are measured by a CMM machine.

Tests 2a and 2b: Complete bearings are installed at the center part of the pin, with one additional bearing at each support. The bearings in the middle are exposed directly to combinations of internal radial tightening from the expanding pin and the external test load. The bearings at the supports are tightened up with the same expanding outwards force as the bearings in the middle.

3.1.2. Complete Bearings Loaded by the Expanding Dual Pin and External Load (Tests 2a and 2b)

The Test 2a involves 4 identical bearings of type SKF GE 80 ES in the same jig at the same time (Reference Figure 5). One bearing is installed at each support, and two are installed between the supports, in such a way that all 4 are exposed equally to the external load. The two in the middle get directly half the external load each, and the two in the supports get half the load as reaction forces. All 4 bearings are exposed to internal, outwards radial expansion from the expanding sleeves. For each step of internal load, the external load is increased stepwise from 0 to 400 and 800 kN, for Tests 2b and 2a, respectively. For each combination of internal load and external load, the required rotational moment to turn the pin connected to the 4 bearings is measured. The two bearings in the supports are exposed to identical internal, outwards radial expansion, but from the outer expanding sleeves. The loads and contact conditions are almost identical for the four bearings. The internal, outwards radial load is achieved by torquing the pin tightening screws. For the Test 2a, the two bearings are supported onto one expanding pin sleeve giving a full contact surface towards the bearings, with one bearing on each sleeve. For the Test 2b, one single bearing is supported onto two separate expanding pin sleeves, giving partly contact surface towards the bearings, with a non-contact area at its center part. The contact combinations between pin and bearing inner ring in Tests 2a and 2b are identical with those for Tests 1a and 1b (Reference Figure 6).

The required static rotational moment to turn the pin installed in the 3 or 4 bearings is measured by a 10 tons capacity hydraulic jack and cell connected to the two end plates through a crossbar, which again are connected to the pin, that is forced to turn; see Figure 7. The moment required for turning the pin is logged against the external load and the tightening screw torques.

Figure 7. Test set-up for Test 2a.

3.2. Cylinder Theory Formulas

Thick-walled cylinder theory [25] is applied to consider the relationship between the inner and outer pressure, and radial displacement between the inner and outer surface of the cylinder thickness. The inner ring of a RSPB is analyzed as an open cylinder, with a constant inner diameter but varying outer diameter along its z-axis. When analyzing a small part of the ring, which means that Δz is small, it gives a small variation in outer radius, Δb.

The strain–stress relationships for thick-walled tube with zero temperature effects are expressed as [25]:

$$\epsilon_r = \frac{1}{E}\left[\sigma_r - \nu(\sigma_\theta + \sigma_z)\right],\ \epsilon_\theta = \frac{1}{E}\left[\sigma_\theta - \nu(\sigma_r + \sigma_z)\right],\ \epsilon_z = \frac{1}{E}\left[\sigma_z - \nu(\sigma_r + \sigma_\theta)\right] = constant \quad (1)$$

where ε_r, ε_θ, and ε_z are radial, tangential, and axial strains; E is the elasticity modulus; ν is Poisson's ratio. The radial, tangential (hoop), and axial stress components σ_r, σ_θ, and σ_z, respectively, can be calculated using the expressions in Equations (2)–(4) [25].

$$\sigma_r = \frac{p_1a^2 - p_2b^2}{b^2 - a^2} - \frac{a^2b^2}{r^2(b^2 - a^2)}(p_1 - p_2) \quad (2)$$

$$\sigma_\theta = \frac{p_1a^2 - p_2b^2}{b^2 - a^2} + \frac{a^2b^2}{r^2(b^2 - a^2)}(p_1 - p_2) \quad (3)$$

$$\sigma_z = \frac{p_1a^2 - p_2b^2}{b^2 - a^2} + \frac{P}{\pi(b^2 - a^2)} = constant \quad (4)$$

where p_1 is internal pressure; p_2 is external pressure; P is the axial force, whose value is zero for an open cylinder; a is the inner radius; b is the outer radius; r is the radius, and the following condition is valid:

$$\sigma_r + \sigma_\theta = \frac{2\left(p_1a^2 - p_2b^2\right)}{b^2 - a^2} = constant \quad (5)$$

In an open cylinder analysis, with no end caps, as for the bearing inner ring, the strain and stress in the z-direction is zero, while the open-end displacement u is expressed as:

$$u_{(open\ end)} = \frac{r}{E(b^2 - a^2)}\left[(1 - \nu)\left(p_1a^2 - p_2b^2\right) + \frac{(1 + \nu)a^2b^2}{r^2}(p_1 - p_2)\right] \quad (6)$$

In these 4 tests, it is expected to have some axial stress in the inner rings due to the axially moving expanding sleeves and the distance rings possibly preventing the inner rings from moving. Tables 2 and 3 show some calculated values for internal pressure and outer surface tangential hoop stress in the bearing inner rings by setting the radially displacement -*u*- equal to the measured expansion by the CMM, from Tests 1a and 1b. The radial stress is zero and the Hoop stress is at its maximum at the ring outer surface, where $r = b$, with highest maximum stress at cross-sections locations "a" and "d", which are at the thinnest ring sections, or sections closest to the ring ends. The calculated values are assumed to be the same for the bearing inner ring in Tests 2a and 2b as for Tests 1a and 1b, if the inner ring is loaded identically, and the bearing is not exposed to external load.

Table 2. Displacement, internal pressure, and hoop stress of inner ring, for Test 1a.

Section Locations [mm]	Non-Lubricated						Lubricated		
	Torque = 15 Nm			Torque = 30 Nm			Torque = 30 Nm		
	u [mm]	p_1 [MPa]	σ_θ [MPa]	u [mm]	p_1 [MPa]	σ_θ [MPa]	u [mm]	p_1 [MPa]	σ_θ [MPa]
a	0.112	84	508	0.347	262	1578	0.483	365	2199
b	0.020	28	82	0.059	84	238	0.091	129	365
c	−0.019	−27	−76	−0.062	−88	−249	−0.076	−108	−306
d	−0.100	−75	−453	−0.327	−247	−1488	−0.442	−344	−2012

Table 3. Displacement, internal pressure, and hoop stress of inner ring, for Test 1b.

Section Locations [mm]	Non-Lubricated						Lubricated		
	Torque = 15 Nm			Torque = 30 Nm			Torque = 30 Nm		
	u [mm]	p_1 [MPa]	σ_θ [MPa]	u [mm]	p_1 [MPa]	σ_θ [MPa]	u [mm]	p_1 [MPa]	σ_θ [MPa]
a	−0.161	−121	−731	−0.315	−238	−1434	0.025	19	114
b	−0.012	−17	−48	−0.017	−24	−68	0.042	60	170
c	0.047	67	190	0.101	144	407	0.047	67	190
d	0.176	133	801	0.350	264	1590	0.044	33	199

4. Discussion of Results

As shown in Figure 4a, Test 1a comprises an internal, radially outwards directional loading of two separate SKF GE 80 ES bearing inner rings, together with the corresponding setup for diameter deformation measurement using a CMM. Each ring was mounted on separate single expanding sleeves as illustrated in Figure 4a Figure 6a. Figures 8–11, from Test 1a and Test 1b, represent how the RSPB inner rings deform with increasing tightening screw torque. It is assumed that the effects from the expanding sleeves will give the same deformation pattern on the inner ring when they are installed in a bearing on an expanding pin, the radial clearance between the inner and outer rings is still not reduced to zero, and the bearing is not exposed to external loads.

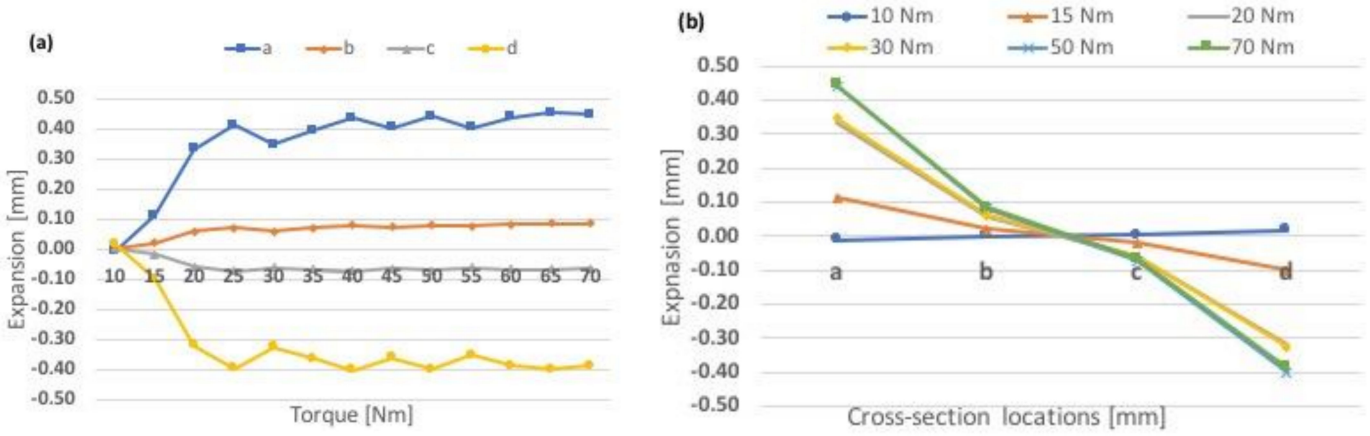

Figure 8. Test 1a—Ring deformations of non-lubricated bearing ring on single sleeve: (**a**) expansion as a function of torque and (**b**) expansion at different cross-section locations.

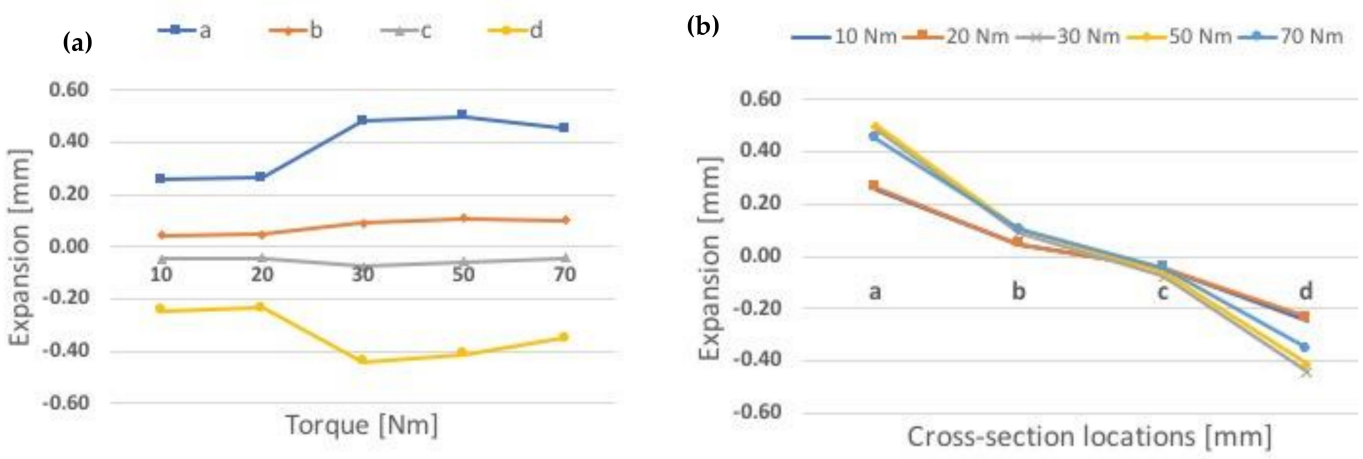

Figure 9. Test 1a—Ring deformations of lubricated bearing ring on single sleeve: (**a**) expansion as a function of torque and (**b**) expansion at different cross-section locations.

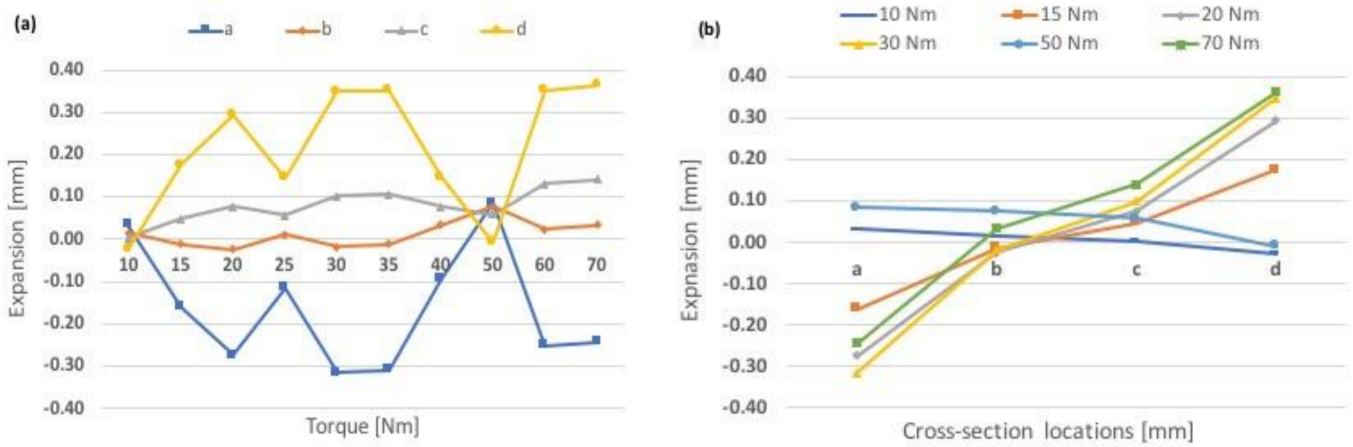

Figure 10. Test 1b—Ring deformations of non-lubricated bearing ring on double sleeve: (**a**) expansion as a function of torque and (**b**) expansion at different cross-section locations.

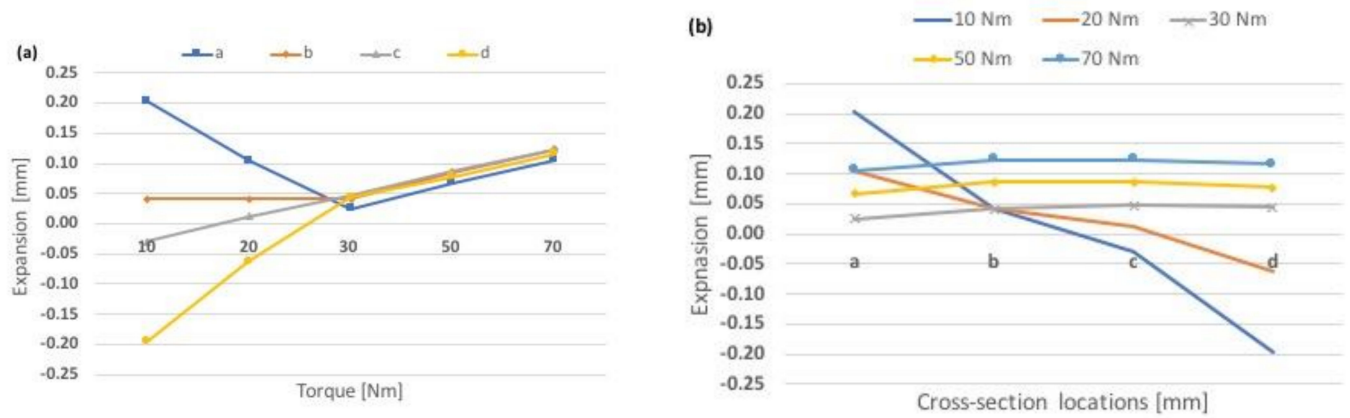

Figure 11. Test 1b—Ring deformations of lubricated single bearing ring on double sleeve: (**a**) expansion as a function of torque and (**b**) expansion at different cross-section locations.

The deformations of the ring on a single sleeve (Test 1a), for dry and lubricated sleeves, can be seen by comparing the results shown in Figures 8 and 9. In the dry case, the ring expands up to 0.410 mm (90.5% of its maximum) at 25 Nm torque, and it stays relatively constant until its maximum of 0.453 mm was reached at 65 Nm torque, at section "a",

which is close to the ring end. At the opposite side of the ring, it contracts to slightly smaller values, or down to 90%. In the lubricated case (Figure 9), the ring expansions and contractions have increased compared to the dry case. Maximum expansion at section location "a" is 0.499 mm at 50 Nm torque, and maximum contraction at same section is 0.442 mm, at 30 Nm torque.

The contraction at the sleeve exit side is almost equal to the expansion at the sleeve entrance side, which stays at or close to 0.40 mm (expansion 347–453 µm and contraction 327–404 µm) at the torque range from 25 Nm up to 70 Nm. The maximum expansion and contraction over the torque range increased slightly with lubricated sleeves but not more than 10%. The average expansion varies up to 3 times higher for the lubricated case compared to the dry case, in the torque range of 20–70 Nm, shown in Figures 12 and 13. For Test 1a, the main expansions and contractions are seen at the ring end sections.

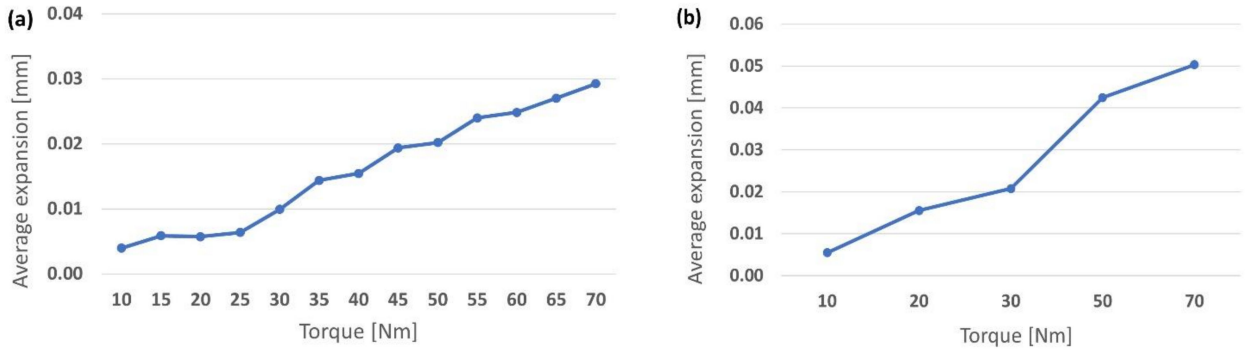

Figure 12. Test 1a—Average ring deformations of bearing rings on (**a**) non-lubricated and (**b**) lubricated single sleeve.

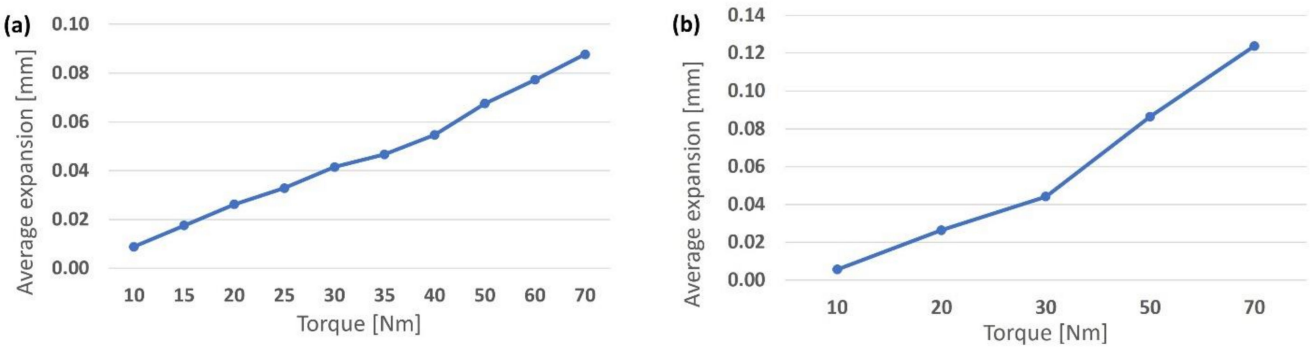

Figure 13. Test 1b—Average ring deformations of bearing rings on (**a**) non-lubricated and (**b**) lubricated double sleeve.

Test 1b was executed in a similar way as Test 1a, but the ring was supported on two separate expanding sleeves at the same time, entering at each ring end, so they leave an unsupported area at the mid part of the ring as illustrated in Figures 4b and 6b. The differences between the deformations of the ring on a double sleeve (Test 1b), for dry and lubricated sleeves, can be seen by comparing the results shown in Figures 10 and 11.

The non-lubricated case shows a serrated shaped curve where the expansion first increases and then decreases to "close to zero" when the accumulated/hysteresis surface contact stress is overcome, with increasing torque. When the ring expands by torquing the bolts and pushing the sleeves, the surface contact friction between ring and sleeve, as well as between sleeve and pin, increase and accumulate. When the torque is increased from 10 to 20 Nm, the expansion at section "d" increased from around 0 to around 0.30 mm (Figure 10a) and decreased almost equally at the opposite ring end, at section "a". The

expansion of the sleeves changed the inner shape of the ring from perfectly cylindrical (within production tolerances) to slightly conical cylinder.

When the torque is increased further up to 25 Nm, the pushing force from the sleeves overcomes the accumulated surface contact stress; it is released, and sliding occurs, possibly between both contact surfaces (ring/sleeve and sleeve/pin) at the same time. When sliding occurs the ring tries to go back from the conical-cylindrical shape to the perfect cylindrical shape, and the contact stress gets more evenly distributed and consequently reduces the ring expansion down to "close to zero" at the "d" section and increases up to "close to zero" at the "a" section. As can be observed from Figures 8a and 10a, the same serrated shaped curve pattern can be seen when increasing the torque from 0 to 70 Nm.

In the lubricated case, it can clearly be seen that the expansion is reduced for all tightening torques, except for the lowest, and it is practically unchanged over the torques range 30–70 Nm. The maximum expansion values for 30, 50, and 70 Nm in the lubricated case are 0.047, 0.087, and 0.124 mm, respectively, compared to the fabric new bearing clearance of 0.072–0.142 mm. As can be observed from the plots in Figure 13, the average expansion varies up to 1.4 times higher for the lubricated case, in the torque range of 20–70 Nm. The lubricated case shows the highest asymmetry at the lowest torque, 10 kN, compared to the non-lubricated case where the asymmetry was around zero. The reason for this is assumed to be that in the lubricated case, the sleeves could move easier due to less friction resistance and thereby expand the ring at the sleeve entrance side that was torqued first (section "a"). When torquing the opposite side (section "d"), part of the asymmetry was eliminated, but not all, while for the non-lubricated case, the torque was lost into increased hysteresis surface contact stress and did not expand the ring until the torque was increased. When the torque increased, the accumulated or hysteresis surface contact stress was overcome, the sleeves slid, and the inner ring shape went back to its normal cylindrical shape or reduced its asymmetry as shown in Figure 11a. The effect of increasing expansion on each side of the inner ring independent of each other, from two different expanding sleeves, forces the ring into a less asymmetric shape. For Test 1b the main expansions and contractions are seen at the ring center sections.

The ring diameter changes at the 4 ring cross-section locations with non-lubricated and lubricated sleeves can be seen in Figures 10 and 11, respectively. The ring average expansion over the rings for Tests 1a and 1b are illustrated in Figures 12 and 13.

The radial expansions for different inner ring cross-sections presented in Figures 8–11 are represented by the deformation -u- in formula (6), and the corresponding inner pressure p_1 and tangential hoop stress σ_θ can be calculated, with the outer pressure $p_2 = 0$, whose results are given in Tables 2 and 3.

Test 2a comprises of two complete RSPBs mounted each on one single sleeve on an expanding pin and loaded both internally (i.e., radially outwards directional loading from expanding the sleeves by torquing the tightening screws) and externally (i.e., radially inwards load from the hydraulic load machine), as shown in Figures 5a and 7. The results from loading the bearing stepwise with internal and external loads and the measure of the required moment to turn the outer ring relatively to the locked inner ring of the bearing on single sleeve are shown in Figure 14. The highest rotational moments are seen at both the lowest and highest tightening torque, 5 and 65 Nm, respectively, and they increase with the increasing external load, for all torque values. The lowest rotational moments occur at 25 and 45 Nm. The reasons for this behavior are understood to be:

- At the lowest torque value, the expansion of the inner ring is zero, as illustrated in Figure 8a, as it would have been in a joint connection with a standard cylindrical pin installed. The required moment to turn the bearing is illustrated in Figure 14a,b, and these values represent fabric new bearings, with a contact surface between the bearing rings that depends on the specific bearing ring tolerance, which is in the range of 72–142 μm. A wide ring tolerance results in a reduced contact area between the two bearing rings and increased contact stresses, with possible accelerated removal of lubrication at the contact areas, followed by increased rotation moment. An increase

of the external load increases the turning moment, as the contact pressure between the rings increases.

- When the torque level is increased to 25 and 45 Nm, the inner ring expands with a slightly serrated shape as illustrated in Figure 8a and changes the ring inner surface shape from cylindrical to conical-cylindrical, with increased opening diameter in one end and reduced opening at the other end. With increased external load, the ring shape is forced back to cylindrical shape, and the total average ring expansion can be seen in Figure 12a. The expansion of the inner ring increases the contact area between the two bearing rings and reduces the contact pressure. These expansion values are below the fabrication tolerances of the bearing, and the required turning moment is reduced, compared to the lowest torque value.
- At the maximum torque value of 65 Nm, the average expansion increases to a level still lower than the bearing internal minimum tolerances (Figure 12a), but the maximum expansion at the inner ring end is 0.45 mm (Figure 8a) which is three times over the bearing maximum tolerance. It is possible that the external load cannot push the ring back from the conical-cylindrical to the original cylindrical shape, and with high contact pressure areas between the two rings, the results show high rotation moment for high torque as well as for low torque.

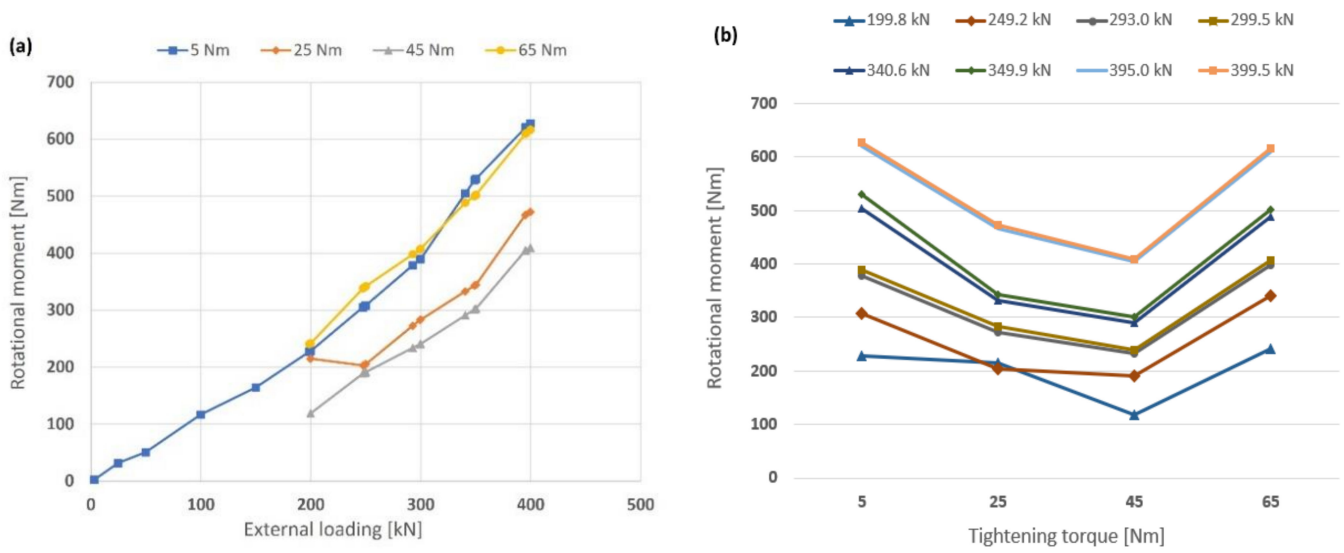

Figure 14. Test 2a—Total rotation moment per bearing, with bearing on single sleeve with (**a**) increasing external load and (**b**) increasing torque level.

Test 2b is performed in a similar way as Test 2a but with one single bearing at the assembly mid part, expanded by two separate sleeves. For the double sleeve setup (Test 2b), the highest rotational moment was clearly only at the lowest tightening torque, 5 Nm, as illustrated in Figure 15, and the remaining torque values in the range of 25–65 Nm did not give any major scattering in moment values. The rotational values are almost identical at torque value 55 Nm, for all external loads, with only a ±9% variation. At the maximum external load, 400 kN, the rotational moment reaches 1903 Nm with 5 Nm torque, and 266–466 Nm with torque values in the range of 15–65 Nm. The high rotational moment for the lowest torque is understood to come from the same reasons as for Test 2a. When the torque is increased to 30 Nm the asymmetry of the ring is reduced to almost zero, see Figure 11. This can be observed because all sections of the ring have increased almost identically (in the range of 0.025–0.05 mm). When the torque further increases from 30 Nm to 70 Nm, the ring stays close to symmetric over its axial length, and the ring diameter increases with increasing torque. Due to the expanding sleeves coming into the ring from both sides, in combination with increasing external load, the ring is continuously forced

back from any conical-cylindrical shape to cylindrical shape; the high contact pressure area between the two rings is avoided, and the high rotation moment does not occur for any increased torque value, within these tests.

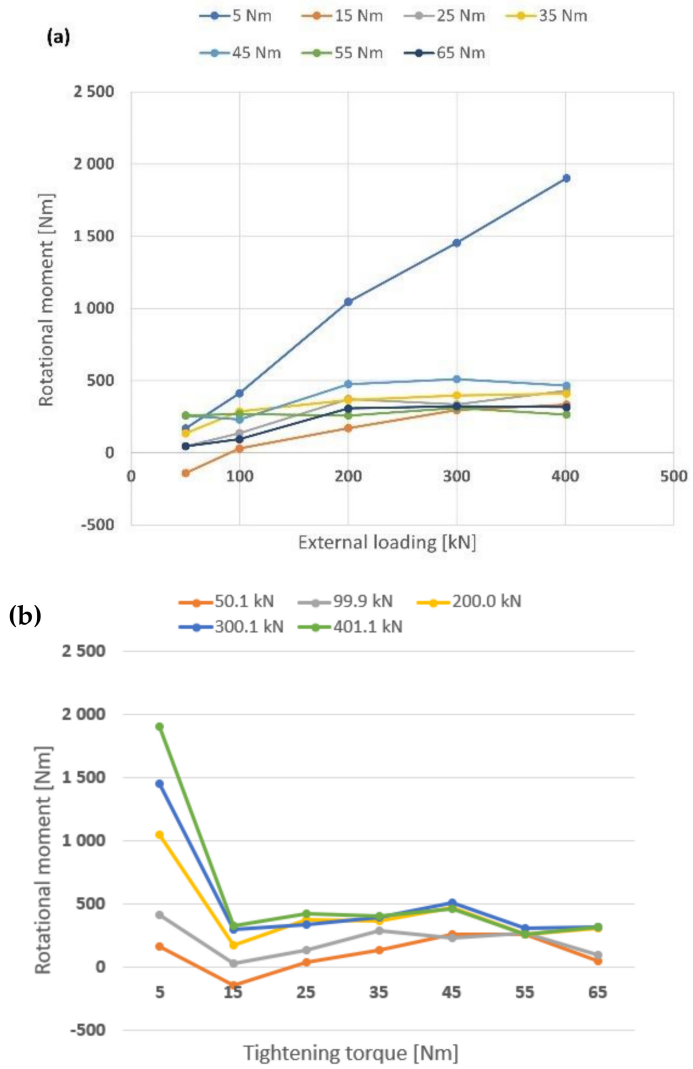

Figure 15. Test 2b—Total rotation moment per bearing with bearing on double sleeves with (**a**) increasing external load and (**b**) increasing torque levels.

A bearing mounted on an expanding pin will experience the inner ring expanding and the contact area between the inner and outer ring increasing with increasing internal load. As a result of external overload, the pin shaft could bend and then also the bearing inner ring, as described by Zhao et al. [18]. Such bending of the pin shaft could lead to increased loss of contact area between pin and inner ring at the ring center, combined with high load from the outer ring at the inner ring center area. This can lead to bending of the inner ring and subsequently brittle crack initiation at the contact areas between inner ring and pin, and inner ring and outer ring.

5. Conclusions

The setup with one bearing on two combined expanding sleeves (designated as Test 2b) clearly shows that a low tightening torque of 5 Nm results in high required rotational moment, compared to higher torques. The 5 Nm torque curve represents a rotational moment close to 1900 Nm at 400 kN external load, and for all other torques at the same external load, the rotational moments are in the range of 266–466 Nm, which is a drop in

rotational moment in the range of 75–86%. The measured rotational moments decrease substantially with only a small increase in tightening torque, due to increased inner ring expansion and reduced high contact pressure areas between the two rings, resulting in lower contact surface stresses between the two bearing rings, with improved lubrication effects. The inner ring expands when the torque levels are increased but not enough to eliminate the internal ring clearances. Thus, the ring contact pressure is reduced when the torque level is increased. For this bearing setup, it can be concluded that expanding the inner ring using expanding pin solutions will lower the total friction forces between the two rings for all external loads. The rotational moment is practically not increasing for each of the torque values within the range from 15 Nm to 65 Nm, within the higher external load range of 200–400 kN.

Following the results of this study, it is open to question whether a RSPB installed on a standard cylindrical pin shaft without the expanding effect will also suffer high friction between the rings and thereby a possibly reduced lifetime compared to the use of an expanding pin solution with a tightening torque above 5–10 Nm. The healthiest set up for the case with one bearing on two sleeves will be to apply a torque level of 20–30 Nm, which gives an equal distributed expansion of the inner ring and an expansion level within or at the lower level of the bearing inner clearance limits of 0.072–0.142 mm, where 20 Nm torque results in a 0.026 mm and 30 Nm in a 0.042 mm ring expansion with dry sleeves, and a 0.026 mm and a 0.044 mm ring expansion for lubricated sleeves, respectively.

The setup with one bearing on one single sleeve (designated as Test 2a) shows that both the lowest and highest torques, 5 Nm and 65 Nm, respectively, result in higher and almost identical rotational moments in the external load range of 200–400 kN. The reason for the high moment at low torque would be the same as in Test 2b, and the high moment at high torque is understood to come from the ring deformation shape, as shown in Test 1a. One side of the inner ring expands and encounters the outer ring and is not pushed back to its cylindrical shape, and high surface contact pressure areas are produced which increase the rotational moment. The healthiest set up for the bearing in this case seems to be with a tightening torque regime in the range of 25–45 Nm with dry sleeves with 0.006 mm and 0.019 mm ring expansion, or 20–40 Nm with lubricated sleeves, and with 0.016 mm and 0.032 mm ring expansion. When lubricating the sleeves, a higher part of the energy input (torque) goes to expand the bearing inner ring, and less is lost in overcoming friction.

Based on this study and its findings, further investigations can be recommended, especially with the use of finite element analysis (FEA) where a wider diameter range of expanding pins can be analyzed, in addition to standard cylindrical pins, in combination with extended laboratory testing. The variables of interest are diameter, bearing type, friction, torque, and external load. In addition, it could be of interest to run bearing fatigue tests with expanding pins.

Author Contributions: Conceptualization, Ø.K.; methodology, Ø.K. and I.B.; software, Ø.K. and I.B.; validation, Ø.K. and H.G.L.; formal analysis, Ø.K.; investigation, Ø.K. and I.B.; resources, Ø.K. and H.G.L.; data curation, Ø.K.; writing—original draft preparation, Ø.K.; writing—review and editing, Ø.K. and H.G.L.; visualization, H.G.L.; supervision, H.G.L.; project administration, Ø.K.; funding acquisition, Ø.K. All authors have read and agreed to the published version of the manuscript.

Funding: The research is conducted as part of Industrial PhD study funded by the Research Council of Norway, placed in Oslo, Norway, web https://www.forskningsradet.no/en/ (accessed on 27 March 2022), Grant nr. 283821. This financial support is highly acknowledged.

Institutional Review Board Statement: Not applicable.

Informed Consent Statement: Not applicable.

Data Availability Statement: Not applicable.

Acknowledgments: We are grateful for all the help, advice, and bearings received from Henrik Tveit at SKF Norway and all the support and guidance from Carl Odvar Hoel at Coba MT, in relation with the tests performed.

Conflicts of Interest: The authors declare no conflict of interest. The authors declare that they have no known competing financial interests or personal relationships that could have appeared to influence the work reported in this paper.

References

1. Myszka, D.H. *Machines and Mechanisms: Applied Kinematic Analysis*, 4th ed.; Pearson Education, Inc.: Old Tappan, NJ, USA, 2012.
2. Salahshour, S.; Karlsen, Ø.; Lemu, H.G. Experimental and numerical studies of stress distribution in an Expanding Pin Joint System. *Appl. Mech.* **2022**, *3*, 46–63. [CrossRef]
3. Ma, J.; Qian, L.; Chen, G.; Li, M. Dynamic analysis of mechanical systems with planar revolute joints with clearance. *Mech. Mach. Theory* **2015**, *94*, 148–164. [CrossRef]
4. Ambrósio, J.; Pombo, J. A unified formulation for mechanical joints with and without clearances/bushings and/or stops in the framework of multibody systems. *Multibody Sys. Dyn.* **2018**, *42*, 317–345. [CrossRef]
5. Fang, C.; Meng, X.; Lu, Z.; Wu, G.; Tang, D.; Zhao, B. Modeling a lubricated full-floating pin bearing in planar multibody systems. *Tribol. Int.* **2019**, *131*, 222–237. [CrossRef]
6. Grant, W.J. Shrink fitting. *Cryogenics* **1972**, *12*, 328–333. [CrossRef]
7. McMillan, M.; Hendry, J.L.; Woolley, A.; Pavier, M.J. Measurement of Partial Slip at the Interface of a Shrink Fit Assembly under Axial Load. *Exp. Mech.* **2018**, *58*, 407–415. [CrossRef]
8. Mouâa, A.; Laghzale, N.E.; Bouzid, A.H. Elastic-plastic stresses in shrink fit with a solid shaft. In Proceedings of the MATEC Web of Conferences EDP Sciences, 14th Congress of Mechanics (CMM2019), Rabat, Morocco, 16–19 April 2019; EDP Sciences: Les Ulis, France, 2019; Volume 286, p. 02001. [CrossRef]
9. Murčinková, Z.; Baron, P.; Pollák, M. Study of the press fit bearing-shaft joint dimensional parameters by analytical and numerical approach. *Adv. Mater. Sci. Eng.* **2018**, *2018*, 2916068. [CrossRef]
10. Lee, D.H.; Kwon, S.J.; Choi, J.B.; Kim, Y.J. Observations of Fatigue Damage in the Press-fitted Shaft under Bending Loads. *Key Eng. Mater.* **2006**, *326*, 1071–1074. [CrossRef]
11. Bondura Technology AS. Available online: https://www.bondura.no/ (accessed on 13 April 2022).
12. Nord-lock Group. Available online: https://www.nord-lock.com/expander-system/ (accessed on 13 April 2022).
13. Karlsen, Ø.; Lemu, H.G. On Modelling Techniques for Mechanical Joints: Literature Study. In *Advanced Manufacturing and Automation IX. IWAMA 2019*; Lecture Notes in Electrical Engineering; Wang, Y., Martinsen, K., Yu, T., Wang, K., Eds.; Springer: Singapore, 2019; p. 634. [CrossRef]
14. Karlsen, Ø.; Lemu, H.G. Fretting fatigue and wear of mechanical joints: Literature study. In Proceedings of the 2nd COTech Conference, Stavanger, Norway, 27–29 November 2019; p. 012015. [CrossRef]
15. Akhtar, M.M.; Karlsen, Ø.; Lemu, H.G. Study of Bondura® Expanding PIN System-Combined Axial and Radial Locking System. *Strojniski Vestnik/J. Mech. Eng.* **2021**, *67*, 625–634. [CrossRef]
16. Berkani, I.; Karlsen, Ø.; Lemu, H.G. Experimental and numerical study of Bondura® 6.6 PIN joints. In Proceedings of the 1st COTech Conference, Stavanger, Norway, 28–29 November 2017; IOP Publishing Ltd: Bristol, UK, 2021; Volume 700, p. 012015. [CrossRef]
17. Öztürk, E.; Yıldızlı, K.; Memmedov, R.; Ülgen, A. Design of an experimental setup to determine the coefficient of static friction of the inner rings in contact with the outer rings of radial spherical plain bearings. *Tribol. Int.* **2018**, *128*, 161–173. [CrossRef]
18. Zhao, X.; Fang, C.; Chen, Y.; Zhang, Y. Failure behaviour of radial spherical plain bearing (RSPB) joints for civil engineering applications. *Eng. Fail. Anal.* **2017**, *80*, 416–430. [CrossRef]
19. Sun, G.; Wu, M.; Yang, Y.; Xue, S. Mechanical properties of radial spherical plain bearing (RSPB) joint with an inserted plate for building structural application–An experimental study. *Structures* **2021**, *33*, 2140–2151. [CrossRef]
20. Fang, X.; Zhang, C.; Chen, X.; Wang, Y.; Tan, Y. Newly developed theoretical solution and numerical model for conformal contact pressure distribution and free-edge effect in spherical plain bearings. *Tribol. Int.* **2015**, *84*, 48–60. [CrossRef]
21. Karlsen, Ø.; Lemu, H.G. Questionnarie-based survey of experiences with the use of expanding PIN systems in mechanical joints. *Results Eng.* **2021**, *9*, 100212. [CrossRef]
22. Karlsen, Ø.; Lemu, H.G. Safety related study of Expanding Pin systems application in lifting and drilling equipment within Construction, Offshore, and Marine sectors. In *IOP Conference Series: Materials Science and Engineering. Proceedings of the 3rd COTech Conference, Stavanger, Norway, 25–26 November 2021*; IOP Publishing Ltd: Bristol, UK, 2021; Volume 1201, p. 012026. [CrossRef]
23. SKF. Available online: https://www.skf.com/group (accessed on 13 March 2022).
24. OVAKO. Available online: https://www.ovako.com/ (accessed on 13 March 2022).
25. Boresi, A.P.; Schmidt, R.J.; Sidebottom, O.M. *Advanced Mechanics of Materials*; Wiley: New York, NY, USA, 1985; Volume 6.